

# Impact of the Atlantic warm pool on United States landfalling hurricanes

Chunzai Wang,<sup>1</sup> Hailong Liu,<sup>1,2</sup> Sang-Ki Lee,<sup>1,2</sup> and Robert Atlas<sup>1</sup>

Received 10 August 2011; revised 1 September 2011; accepted 4 September 2011; published 7 October 2011.

[1] The 2010 Atlantic hurricane season was extremely active, but no hurricanes made landfall in the United States, raising a question of what dictated the hurricane track. Here we use observations from 1970–2010 (also extending back to 1950) and numerical model experiments to show that the Atlantic warm pool (AWP) – a large body of warm water comprised of the Gulf of Mexico, the Caribbean Sea and the western tropical North Atlantic – plays an important role in the hurricane track. An eastward expansion of the AWP shifts the hurricane genesis location eastward, decreasing the possibility for a hurricane to make landfall. A large AWP also induces barotropic stationary wave patterns that weaken the North Atlantic subtropical high and produce the eastward steering flow anomalies along the eastern seaboard of the United States. Due to these two mechanisms, hurricanes are steered toward the northeast without making landfall in the United States. Although the La Niña event in the Pacific may be associated with the increased number of Atlantic hurricanes, its relationship with landfalling activity has been offset in 2010 by the effect of the extremely large AWP. **Citation:** Wang, C., H. Liu, S.-K. Lee, and R. Atlas (2011), Impact of the Atlantic warm pool on United States landfalling hurricanes, *Geophys. Res. Lett.*, 38, L19702, doi:10.1029/2011GL049265.

## 1. Introduction

[2] Almost all of the severest hurricane-related loss and damage occur when hurricanes make landfall. Thus, a better understanding of factors controlling hurricane's landfall is both scientifically and socially important. The Atlantic hurricane season officially starts on June 1 and ends on November 30. An average hurricane season, based on the data from 1950–2000 without considering short-lived storms [Landsea *et al.*, 2010], has 9.6 named storms and an accumulated cyclone energy (ACE) index of 96.1 (a measure of overall tropical cyclone activity with the unit of  $10^4 \text{ kt}^2$ ) [e.g., Klotzbach and Gray, 2006]. Of these 9.6 storms, 5.9 are hurricanes (categories 1–5) and 2.5 are major hurricanes (categories 3–5). The average ratio between U. S. landfalling hurricanes and total hurricanes is about 25%. However, an active hurricane season does not necessarily mean more U. S. landfalling hurricanes because the hurricane track is determined by both the hurricane internal dynamics and large-scale climate variations.

<sup>1</sup>Atlantic Oceanographic and Meteorological Laboratory, NOAA, Miami, Florida, USA.

<sup>2</sup>Cooperative Institute for Marine and Atmospheric Studies, University of Miami, Miami, Florida, USA.

[3] The 2010 Atlantic hurricane season had 19 named storms, 12 hurricanes, 5 major hurricanes and an ACE index of 166.3, all of which indicate that the 2010 season was extremely active. However, for the 2010 hurricane season, not a single hurricane made landfall in the United States. As shown in Figure 1a, there were 6 tropical storms and hurricanes that made landfall in Central America, and one tropical storm that made landfall in Florida. But, these were largely short-lived tropical storms that formed in the Caribbean Sea. Excluding those that formed in the Caribbean Sea, Figure 1b shows that tropical storms and hurricanes formed in the main development region (MDR) moved northwestward and then recurved northeastward to the subtropical North Atlantic, with the exception of two storms that dissipated near the MDR.

[4] In this paper, we mainly focus on the tropical cyclones (TCs) that formed in the MDR and investigate why and how an active hurricane season can occur without a hurricane to make landfall in the United States. Using observations and numerical model experiments, we emphasize the role of the Atlantic warm pool (AWP) in the hurricane track. The paper also discusses the impact of other climate phenomena on the hurricane track.

## 2. Data Sets and Model Experiments

[5] The first data set is the NOAA extended reconstructed SST version 3 [Smith *et al.*, 2008], and the second one is the NCEP-NCAR reanalysis [Kalnay *et al.*, 1996]. Hurricane data are from HURDAT reanalysis database ([http://www.aoml.noaa.gov/hrd/data\\_sub/re\\_anal.html](http://www.aoml.noaa.gov/hrd/data_sub/re_anal.html)). What we use here includes the ACE, all hurricanes, major hurricanes, total named storms, and TC track density. The ACE index is calculated by summing the squares of the estimated maximum sustained wind of every TC, at six-hour intervals. Based on the best-track hurricane data of HURDAT, TC track density is computed by counting the number of TCs passing through each  $5^\circ \times 5^\circ$  grid box for a given calendar year. Since the hurricane data are relatively reliable after the satellite measurements, here we use the hurricane data from 1970 to 2009. We also use the hurricane data from 1950 to 2009 and get the similar results (Figures 3 and Figure S9 in the auxiliary material).<sup>1</sup> The 2010 hurricane data is from NOAA National Hurricane Center (<http://www.nhc.noaa.gov/2010atlan.shtml>).

[6] The NCAR community atmospheric model version 3.1 (CAM3) is forced by the Hadley Centre SST (HadSST) on a  $1^\circ \times 1^\circ$  resolution. Based on the HadSST of 1949–2001, we compute monthly SST composites for large AWP (six large AWP years are 1952, 1958, 1969, 1987, 1995, and

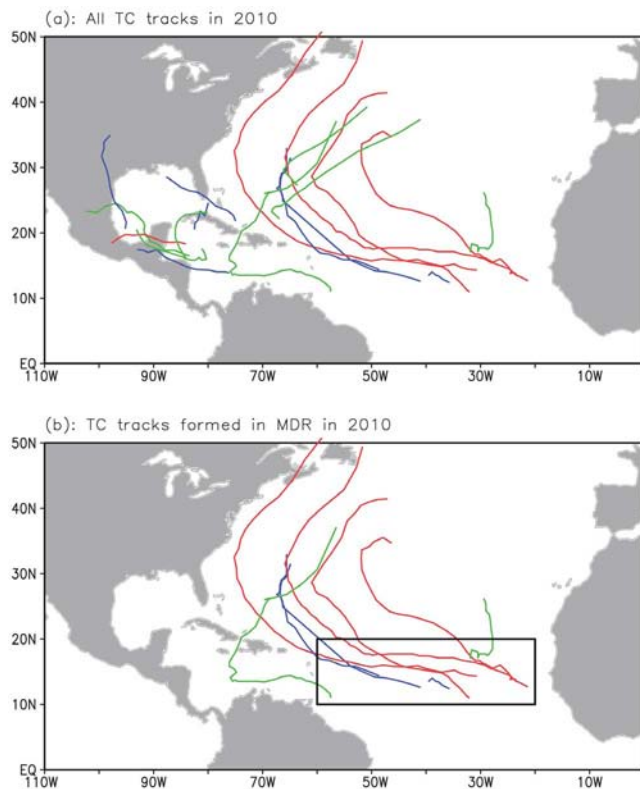


**Figure 1.** TC tracks in the 2010 Atlantic hurricane season. Shown are (a) all TCs in the 2010 season and (b) TCs that formed in the MDR indicated by the box ( $10^{\circ}\text{N}$ – $20^{\circ}\text{N}$ ,  $60^{\circ}\text{W}$ – $20^{\circ}\text{W}$ ). TCs that reached major hurricane (Category 3–5) intensity are in red color and TCs that reached Category 1–2 hurricane intensity are in green color.

1998) and small AWP (seven small AWP years are 1971, 1974, 1975, 1976, 1984, 1986, and 1992). We use these SST composites to perform two sets of ensemble model simulations: large AWP (LAWP) and small AWP (SAWP). In the LAWP run, the twelve-monthly SSTs for the large AWP composites are used in the AWP region for forcing CAM3, while the monthly climatology is specified for the rest of the global ocean. In the set of the SAWP simulation, CAM3 is forced by the small AWP monthly SST composites in the AWP region and climatological SST elsewhere. For the detailed model experiments, see Wang *et al.* [2008a].

### 3. Role of the AWP in the Hurricane Track

#### 3.1. Observational Results

[7] The influence of the AWP on the TC track operates through at least two ways. The first one is the AWP-related shift of the TC genesis location. The AWP in August–October (ASO) expands toward the east during large AWP years, whereas it contracts during small AWP years (Figures 2a and 2b). The eastward shift of warm water and its associated reduction of vertical wind shear result in increased TC activity [Bell and Chelliah, 2006; Kossin and Vimont, 2007; Wang *et al.*, 2008b]. As shown in Figures 2a and 2b, more TCs are formed east of  $40^{\circ}\text{W}$  in large AWP years due to the increased SST and atmospheric convective instability there. Figures 2c and 2d show the tracks of TCs that formed in the MDR for large and small AWP, with blue (red) color representing TCs formed in the east (west) of  $40^{\circ}\text{W}$ . Based on Figures 2c and 2d, the ratios of U. S. landfalling TCs (i.e., the number of landfalling TCs divided by the total number of TCs) in the east and west of  $40^{\circ}\text{W}$  are 13.2% and 29.0%, respectively. This indicates that TCs formed further eastward have less opportunity to make landfall in the United States.

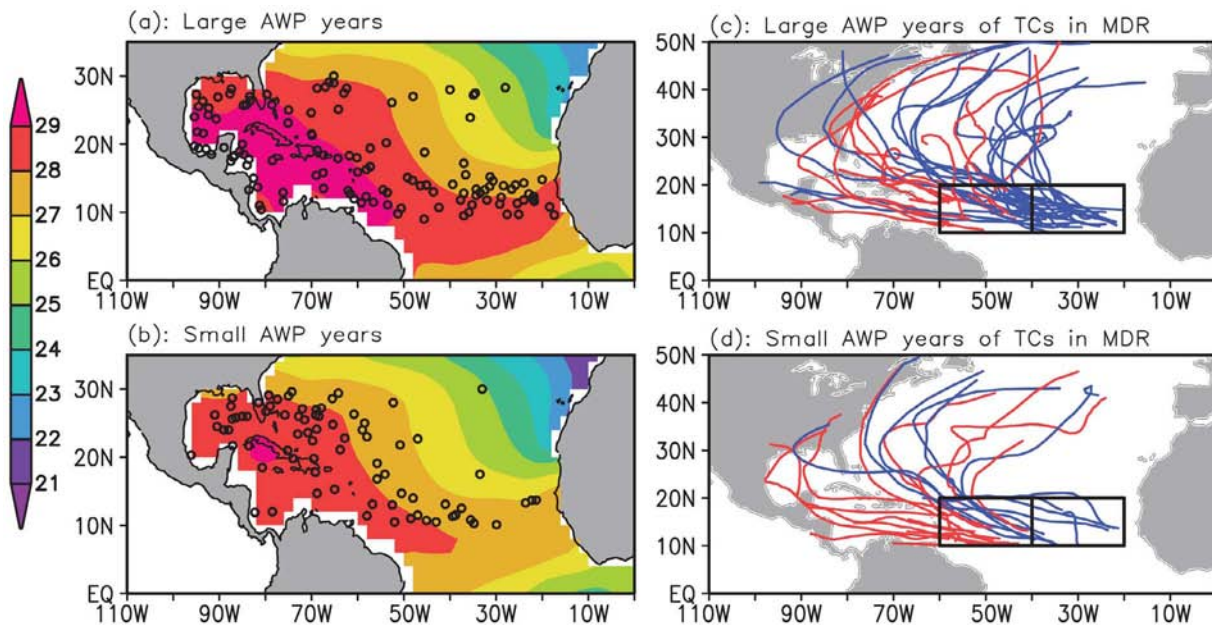


**Figure 2.** The TC genesis location, TC track and AWP variability. Shown are the TC genesis location (dots) and SST (shading) for (a) large and (b) small AWP years and the tracks of TCs that formed in the MDR for (c) large and (d) small AWP. Based on the data from 1970 to 2009, the top and bottom quartiles of the ASO AWP index are identified as large and small AWP years, respectively. The composites of SST for large and small AWP years are then computed. The dots represent the location of all TCs formed southward of  $30^{\circ}\text{N}$  in large (126 TCs) and small (79 TCs) AWP years. In Figures 2c and 2d, 38 (31) TCs are formed in the east (west) of  $40^{\circ}\text{W}$  with 5 (9) TCs making landfall in the United States.

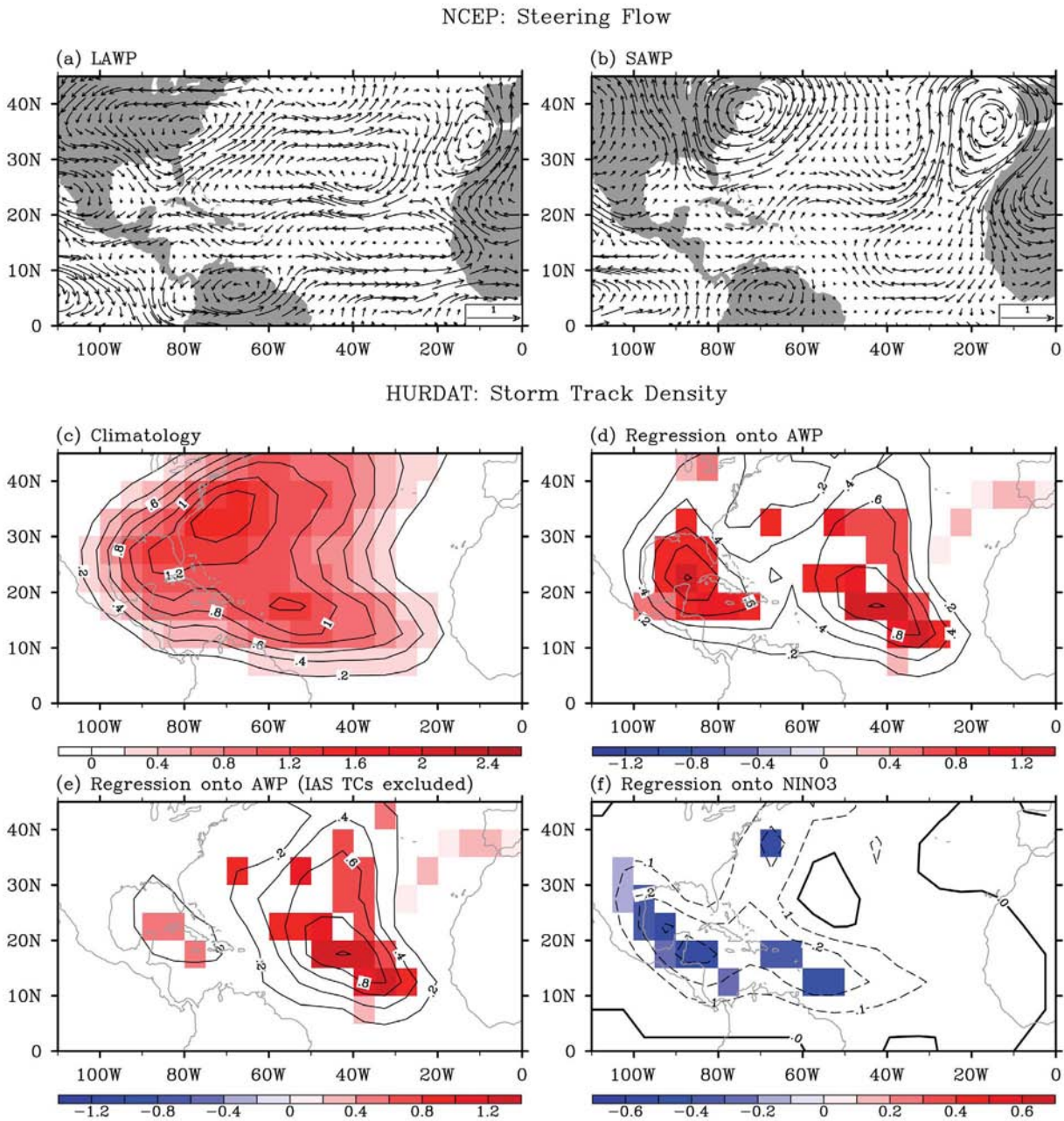


**Figure 3.** The TC steering flow and TC track density, and their relationship with AWP and ENSO variability during ASO. Shown are the TC steering flow anomalies ( $\times 10^3$  hPa m/s) for (a) large and (b) small AWP years, (c) the climatological mean of TC track density (the number), (d) the regression coefficient (the number per 100%) of TC track density onto AWP index, (e) the regression coefficient (the number per 100%) of TC track density onto AWP index with IAS TCs excluded, and (f) the regression coefficient (the number per  $^{\circ}\text{C}$ ) of TC track density onto Nino3 index. In Figures 3d–3f, the regression coefficients higher than the 95% significant level are shaded. The AWP index is calculated as the anomalies of the area of SST warmer than  $28.5^{\circ}\text{C}$  divided by the climatological ASO AWP area. Based on the data from 1970 to 2009, the top and bottom quartiles of the AWP index are identified as large and small AWP years, respectively. The steering flow anomalies are computed by compositing the vertically-averaged wind anomalies from 850 hPa to 200 hPa for large and small AWP years.

Therefore, a large AWP shifts the TC genesis location eastward which increases the possibility for a hurricane to move northward without making landfall in the United States.

[8] The result is consistent with the southeastward shift of the genesis location for the strongest Atlantic meridional mode (AMM) years [Kossin and Vimont, 2007; Kossin et al.,

2010]. The AMM is a climate mode of variability intrinsic to the tropical coupled ocean-atmosphere system and involves a positive feedback between surface wind, evaporation and SST. Thus, a strong AMM may be associated with or induce a large AWP, resulting in the eastward shift of the TC genesis location.

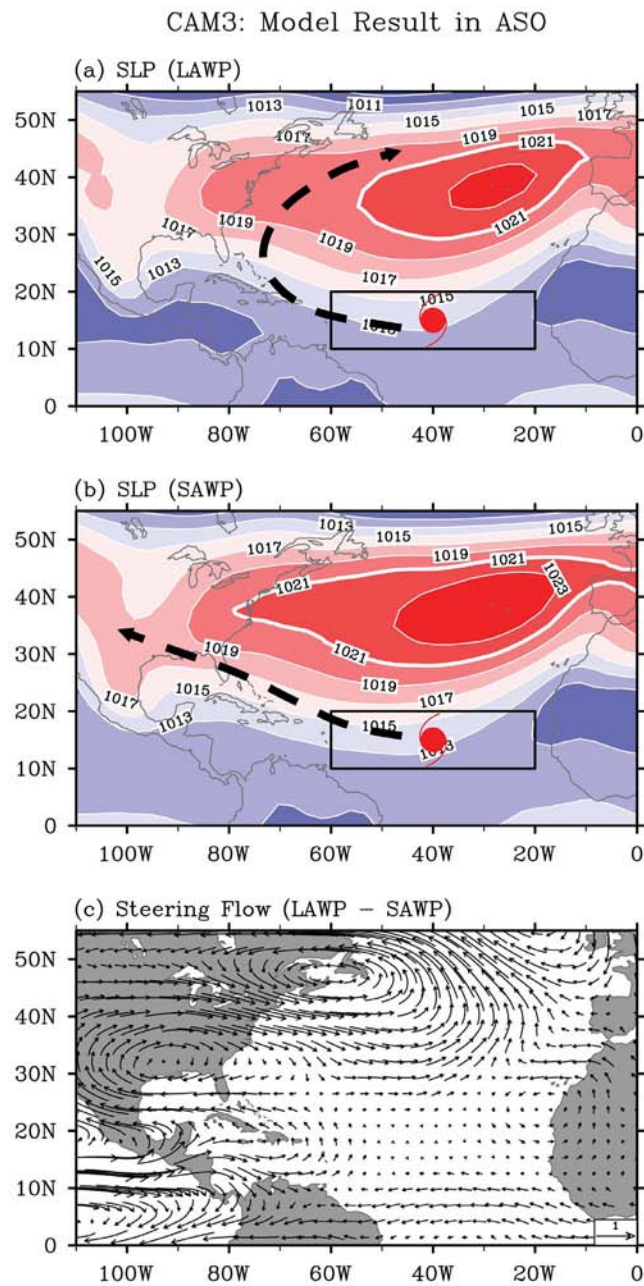


**Figure 4.** The simulated effect of the AWP on the NASH from the CAM3 runs during ASO. Shown are the SLPs for the (a) large AWP (LAWP) run, (b) small AWP (SAWP) run and (c) steering flow difference between LAWP and SAWP runs. The steering flow ( $\times 10^3$  hPa m/s) is calculated as the vertically-averaged wind from 850 hPa to 200 hPa. The dashed arrows are schematically drawn, illustrating the hurricane track if a hurricane forms in the MDR.

[9] The second one is that the AWP induces the changes of atmospheric circulation pattern to influence the TC track. The movement of TCs or the TC track is mainly steered by the surrounding environmental flow in the troposphere and modified by the beta-effect. An integrated flow through a layer of the atmosphere is usually defined as the TC steering flow [e.g., Dong and Neumann, 1986]. To examine the influence of the AWP on the TC steering flow, we calculate the

steering flow anomalies for large and small AWP years. For large AWP years, Figure 3a displays an anomalous cyclonic flow over the eastern U. S. and an anomalous anticyclonic flow over Mexico and the eastern North Pacific. Associated with these patterns are the southeastward flow anomalies in the Gulf of Mexico and the northeastward flow anomalies in the southeast seaboard of the U. S. (Figure 3a). The opposite is true for small AWP years (Figure 3b). Thus, observational data show that a large (small) AWP is associated with the steering flow which is unfavorable (favorable) for a hurricane to make landfall in the United States. Additionally, the steering flow anomalies in neutral AWP years are very small in comparison with large/small AWP years (Figure S1), indicating that AWP variability plays a key role for the TC steering flow change.

[10] The relationship between the AWP and TC tracks is further investigated by using the TC track density data from 1970 to 2009. The climatological mean of TC track density is shown in Figure 3c. Consistent with that by Xie *et al.* [2005], the center of maximum TC density is located in the western subtropical North Atlantic, reflecting that most of TCs form in the tropical North Atlantic and move northwestward. The impact of the AWP on the TC track is examined by linearly regressing TC track density onto the AWP index (Figure 3d). The regression is positive in the entire North Atlantic, reflecting that a large (small) AWP increases (decreases) Atlantic hurricane activity overall [Wang *et al.*, 2006]. The regressed map also shows two maxima: one is in the Intra-Americas Sea (IAS), i.e., the Gulf of Mexico and the Caribbean Sea, and the other is located in the subtropical central North Atlantic. The maximum regression in the IAS is due to TCs that form in the IAS typically during the early and late season as in the 2010 season (Figure 1). To confirm the result, we exclude all TCs that form in the IAS from the hurricane data and recalculate the regression. As shown in Figure 3e, the maximum regression in the IAS almost disappears. The maximum regression in the subtropical central North Atlantic is oriented in a nearly south-to-north direction far away from the U. S. eastern seaboard. This indicates that hurricanes tend to move northward to the subtropical North Atlantic Ocean instead of making landfall in the U. S. during large AWP years. The distributions of TC track density in large and small AWP years also support the results reported here (Figures S2 and S3).

### 3.2. Modeling Results

[11] We next use CAM3 to show that the AWP affects the TC track via the AWP-induced steering flow change. In the tropical North Atlantic, TCs usually move toward the west with a slight poleward component due to an axis of high pressure called the North Atlantic subtropical high (NASH) that extends east-west poleward of TCs. On the equatorward side of the NASH, the easterly trade winds prevail. However, if the NASH is weak and/or shifts northeastward, TCs may turn poleward and then recurve toward the east [e.g., Liu and Fearn, 2000; Elsner *et al.*, 2000]. On the poleward side of the NASH, the westerly winds prevail thus steering TCs back to the east. Hence, both the position and strength of the NASH can determine and change the movement of TCs.

[12] The CAM3 simulated NASHs from the ensemble LAWP and SAWP model runs are shown in Figure 4. A

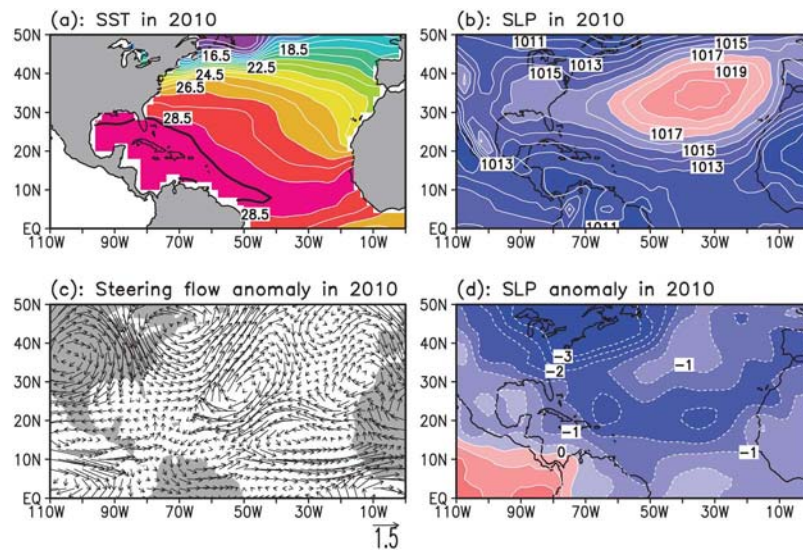


**Figure 5.** The AWP, NASH and steering flow during ASO of 2010. Shown are (a) the SST, (b) the SLP, (c) the steering flow anomalies ( $\times 10^3$  hPa m/s), and (d) the SLP in ASO of 2010 minus climatological ASO SLP. The AWP is defined by SST warmer than  $28.5^\circ\text{C}$ . The dark contour in Figure 5a represents the climatological ASO AWP.

comparison of Figures 4a and 4b shows that the sea level pressure (SLP) associated with the NASH is significantly decreased (increased) in response to a large (small) AWP. The contour of 1021-hPa for the LAWP run stays in the eastern subtropical North Atlantic, whereas its counterpart for the SAWP run extends westward to the east coast of the United States. Therefore, AWP variability affects both the strength and position of the NASH.

[13] The steering flow patterns associated with the LAWP and SAWP model runs show an anomalous anticyclonic flow centered over the southeastern U. S. and an anomalous cyclonic flow immediately northeastward (Figure 4c). The simulated steering flow patterns are consistent with observations although the centers of these steering flow patterns are located slightly northeastward in comparison with the observational results of Figure 3. As demonstrated by using a simple two-level atmospheric model [Lee *et al.*, 2009], these patterns are the AWP-induced barotropic stationary waves in the boreal summer/fall. These AWP-forced stationary waves produce the eastward flow anomalies along the eastern seaboard of the U. S. that prevent hurricanes from making landfall in the United States. As schematically drawn in Figures 4a and 4b, the LAWP-induced northeastward retreat of the NASH will allow a more frequent northeastward recurvature of hurricanes, whereas the SAWP-induced NASH distribution creates a more favorable condition for hurricanes to make landfall in the United States. In other words, a large AWP does not allow the NASH to extend far west, meaning that hurricanes likely would be steered around NASH's edge to the northeast instead of making landfall in the United States.

#### 4. Impact of Other Climate Factors and the 2010 Hurricane Season

[14] It is well-known that ENSO can remotely influence Atlantic hurricane activity: a La Niña (El Niño) event in the tropical Pacific increases (decreases) the frequency of Atlantic

hurricanes [e.g., Bell and Chelliah, 2006]. ENSO's impact on the hurricane track is shown by regressing TC track density onto the Nino3 index (Figure 3f). The significant negative regression is located near the IAS, suggesting that cold (warm) SST anomalies in the tropical Pacific increase (decrease) TC density in the IAS. In other words, a La Niña (El Niño) event in the Pacific tends to enhance (suppress) the possibility for a hurricane to make landfall in Central America, Caribbean Islands, and the southeastern United States.

[15] Now, with the relationships among the AWP, ENSO, NASH and hurricane track from historical data and model experiments, it is quite straightforward to explain why the 2010 hurricane season was so active, but without a land-falling hurricane in the United States. The AWP during ASO of 2010 was extremely large, being about 2.2 times larger than its climatological mean (Figure 5a). 2010 was also a La Niña year: cold SST anomalies covered the equatorial central and eastern Pacific during the 2010 hurricane season. A combination of the local effect of the large AWP and remote influence of the La Niña condition in the Pacific resulted in an active 2010 season. However, the large AWP in 2010 weakened the NASH and pushed the NASH northeastward (Figures 5b and 5d). The negative SLP anomalies in the southwestern tropical North Atlantic indicated a northeastward retreat of the NASH. As shown and discussed earlier, the weakening and the northeastward shift of the NASH tend to make a hurricane move northward and northeastward. Therefore, although climate phenomena in 2010 tended to increase the number of Atlantic hurricanes, the large AWP in 2010 weakened the NASH and prevented the NASH from extending far west, resulting in hurricanes being steered around NASH's edge to the northeast instead of making landfall in the United States. The steering flow anomalies in 2010 showed a cyclonic flow in the western North Atlantic and an anticyclonic flow in the southeastern U. S. (Figure 5c). The cyclonic and anticyclonic steering

flow patterns in 2010 were similar to the observed ones during the past decades (Figures 3a and 3b) and the modeling result (Figure 4c). It is clear that the steering flow anomalies in 2010 were favorable for TCs to move north-westward and then recurve northeastward.

[16] Figures 3f and S4c clearly show that a La Niña event tends to increase the possibility of landfall in the southeastern U. S. and potentially decrease recurving hurricanes. This suggests that the 2010 La Niña event in the tropical Pacific should have favored Atlantic hurricanes to make a landfall, which is not the case in the 2010 hurricane season. Therefore, it can be concluded that the influence of the La Niña event in 2010 may have been offset by an extremely large AWP which displayed the NASH to the northeast of its climatological location.

[17] Other climate phenomena, which may also contribute to Atlantic hurricane activity, include the North Atlantic oscillation (NAO) [e.g., Elsner *et al.*, 2000; Kossin *et al.*, 2010] and the Atlantic multidecadal oscillation (AMO) [e.g., Goldenberg *et al.*, 2001]. As shown in Figure S6, the NAO index is extremely low in the year of 2010 relative to its climatology. Since the NAO index represents variations of the Icelandic low and the NASH, the low NAO index in 2010 may be associated with a weakening of the NASH. This seems to suggest that the observed weakening and northeastward movement of the NASH during 2010 in Figure 5 may also include the effect of the NAO. However, the relationship of the NAO with TC track density is not significant except in the extratropics (Figure S7a). Regarding AMO's impact, it has been shown that the AWP serves as a link between the AMO and Atlantic hurricane activity [Wang *et al.*, 2008b]. Therefore, the influence of the AMO on hurricanes may operate through the mechanism of the AWP-induced atmospheric changes. This is supported by the similar regressed TC track density patterns for the AMO (Figures S7b and S7c) and the AWP (Figures 3d and 3e).

## 5. Summary and Discussion

[18] The paper shows that the AWP affects the Atlantic TC track, in addition to the increase in the number of TCs. A large AWP shifts the TC genesis location eastward, so it increases the chance for a TC to move northward without making landfall in the United States. A large AWP also weakens the NASH and thus induces the northward and northeastward steering flow anomalies, which steer hurricanes away from the United States. Other climate phenomena such as ENSO and the NAO cannot explain the lack of landfalling hurricanes in 2010. An implication of this study is that a better prediction of climate variability can help improve the U. S. landfalling hurricane outlook.

[19] In this paper, we use the data from 1970–2009 to identify large AWP years by the top quartiles of the AWP index (1987, 1998, 2001, 2003, 2004, 2005, 2006, 2007, 2008, and 2009) and small AWP years by the bottom quartiles of the AWP index (1971, 1974, 1975, 1976, 1982, 1984, 1985, 1986, 1992, and 1994). These ten large and small AWP years are respectively associated with 31 and 13 hurricanes that form in the MDR, of which 7 and 5 hurricanes make landfall in the United States. This indicates that (1) the large AWP increases the number of hurricanes formed in

the MDR, and (2) but the large AWP decreases the ratio of U. S. landfalling hurricanes by about 40%.

[20] The factors controlling the TC track are complicated, determined by the TC internal dynamics and large-scale climate as well as synoptic weather patterns. As an example, 2005 was a busy season and also had more landfalling hurricanes. Five of fifteen hurricanes in 2005 made landfall in the United States. Four hurricanes were formed in the MDR in 2005. Of these four hurricanes, one made landfall in Central America and the other three moved northward without landfalling in the United States. The AWP in 2005 was large although it was smaller than that in 2010 (Figure S8a). The SLP anomalies are negative in the AWP region, but near neutral over the U. S. (Figure S8d). The lack of SLP response over the U. S. may be due to different teleconnections induced by different AWP heating patterns or different latitudinal positions of the subtropical jet [Lee *et al.*, 2009]. Associated with the SLP distributions are the steering flow anomalies showing the westward and northwestward flows in the tropical North Atlantic and the AWP region (Figure S8c), which were favorable for hurricanes to make landfall.

[21] **Acknowledgments.** We thank S. Aberson, F. Marks, C. Landsea and anonymous reviewers for their comments and suggestions. This work was supported by NOAA Climate Program Office and the base funding of NOAA AOML.

[22] The Editor thanks the two anonymous reviewers for their assistance in evaluating this paper.

## References

- Bell, G. D., and M. Chelliah (2006), Leading tropical modes associated with interannual and multidecadal fluctuations in North Atlantic hurricane activity, *J. Clim.*, *19*, 590–612, doi:10.1175/JCLI3659.1.
- Dong, K., and C. J. Neumann (1986), The relationship between tropical cyclone motion and the environmental geostrophic flows, *Mon. Weather Rev.*, *114*, 115–122, doi:10.1175/1520-0493(1986)114<0115:TRBTCM>2.0.CO;2.
- Elsner, J. B., K.-B. Liu, and B. Kocher (2000), Spatial variations in major U.S. hurricane activity: Statistics and a physical mechanism, *J. Clim.*, *13*, 2293–2305, doi:10.1175/1520-0442(2000)013<2293:SVIMUS>2.0.CO;2.
- Goldenberg, S. B., C. Landsea, A. M. Mestas-Nunez, and W. M. Gray (2001), The recent increase in Atlantic hurricane activity, *Science*, *293*, 474–479, doi:10.1126/science.1060040.
- Kalnay, E., et al. (1996), The NCEP/NCAR 40-year reanalysis project, *Bull. Am. Meteorol. Soc.*, *77*, 437–471, doi:10.1175/1520-0477(1996)077<0437:TNYRP>2.0.CO;2.
- Klotzbach, P. J., and W. M. Gray (2006), Causes of the unusually destructive 2004 Atlantic basin hurricane season, *Bull. Am. Meteorol. Soc.*, *87*, 1325–1333, doi:10.1175/BAMS-87-10-1325.
- Kossin, J. P., and D. J. Vimont (2007), A more general framework for understanding Atlantic hurricane variability and trends, *Bull. Am. Meteorol. Soc.*, *88*, 1767–1781, doi:10.1175/BAMS-88-11-1767.
- Kossin, J. P., S. J. Camargo, and M. Sitkowski (2010), Climate modulation of North Atlantic hurricane tracks, *J. Clim.*, *23*, 3057–3076, doi:10.1175/2010JCLI3497.1.
- Landsea, C. W., G. A. Vecchi, L. Bengtsson, and T. R. Knutson (2010), Impact of duration thresholds on Atlantic tropical cyclone counts, *J. Clim.*, *23*, 2508–2519, doi:10.1175/2009JCLI3034.1.
- Lee, S.-K., C. Wang, and B. E. Mapes (2009), A simple atmospheric model of the local and teleconnection responses to tropical heating anomalies, *J. Clim.*, *22*, 272–284, doi:10.1175/2008JCLI2303.1.
- Liu, K.-B., and M. L. Fearn (2000), Reconstruction of prehistoric landfall frequencies of catastrophic hurricanes in northwestern Florida from Lake sediment records, *Quat. Res.*, *54*, 238–245, doi:10.1006/qres.2000.2166.
- Smith, T. M., R. W. Reynolds, T. C. Peterson, and J. Lawrimore (2008), Improvements to NOAA's Historical Merged Land-Ocean Surface Temperature Analysis (1880–2006), *J. Clim.*, *21*, 2283–2296, doi:10.1175/2007JCLI2100.1.

- Wang, C., D. B. Enfield, S.-K. Lee, and C. W. Landsea (2006), Influences of the Atlantic warm pool on Western Hemisphere summer rainfall and Atlantic hurricanes, *J. Clim.*, *19*, 3011–3028, doi:10.1175/JCLI3770.1.
- Wang, C., S.-K. Lee, and D. B. Enfield (2008a), Climate response to anomalously large and small Atlantic warm pools during the summer, *J. Clim.*, *21*, 2437–2450, doi:10.1175/2007JCLI2029.1.
- Wang, C., S.-K. Lee, and D. B. Enfield (2008b), Atlantic warm pool acting as a link between Atlantic multidecadal oscillation and Atlantic tropical cyclone activity, *Geochem. Geophys. Geosyst.*, *9*, Q05V03, doi:10.1029/2007GC001809.
- Xie, L., et al. (2005), Climatology and interannual variability of North Atlantic hurricane tracks, *J. Clim.*, *18*, 5370–5381, doi:10.1175/JCLI3560.1.
- 
- R. Atlas and C. Wang, Atlantic Oceanographic and Meteorological Laboratory, NOAA, 4301 Rickenbacker Cswy., Miami, FL 33149, USA. (chunzai.wang@noaa.gov)
- S.-K. Lee and H. Liu, Cooperative Institute for Marine and Atmospheric Studies, University of Miami, Miami, FL 33149, USA.

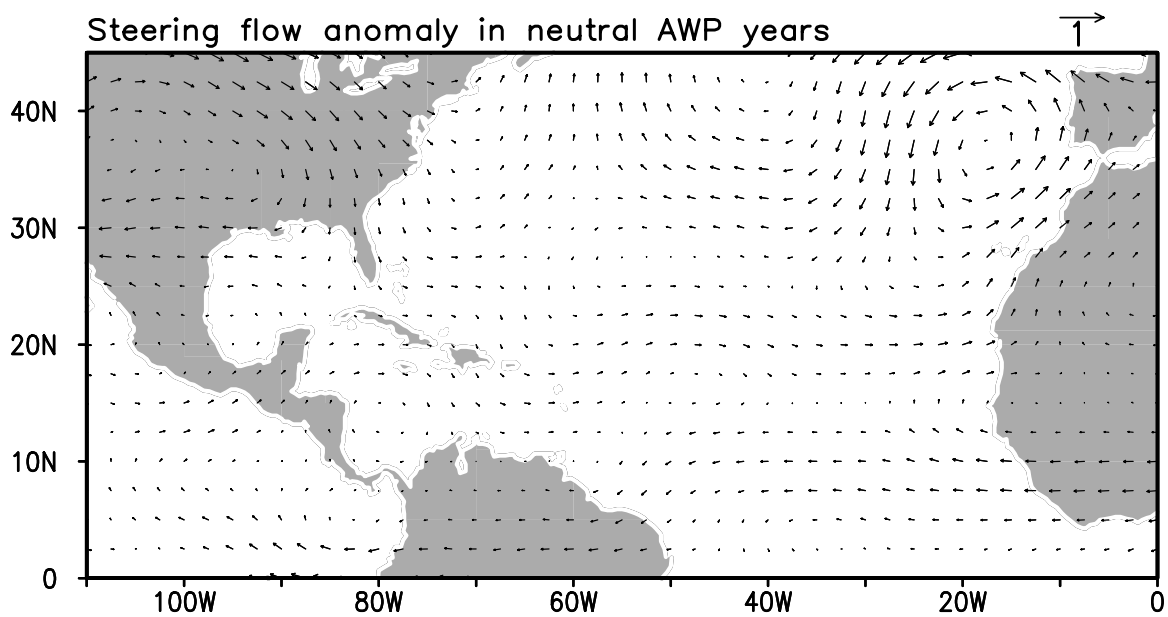


**Figure S1.** The TC steering flow anomalies during ASO for neutral AWP years. Based on the data from 1970 to 2009, the top and bottom quartiles of the AWP index are identified as large and small AWP years, respectively and the middle quartiles are defined as neutral AWP years. The steering flow anomalies are computed by compositing the vertically-averaged wind anomalies from 850 hPa to 200 hPa for neutral AWP years.

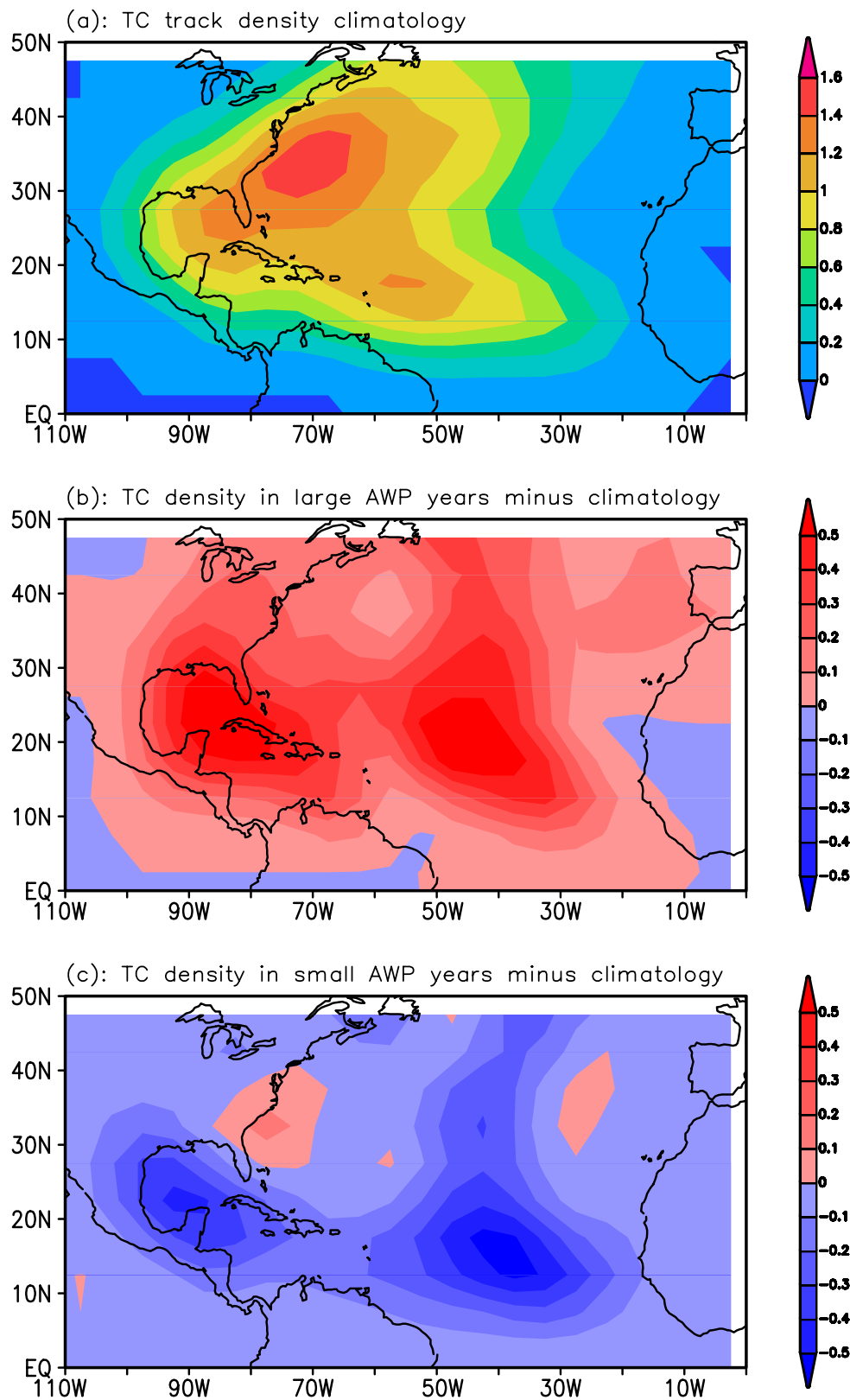


**Figure S2.** TC track density and AWP variability during ASO. Shown are (a) climatological TC track density, (b) TC track density in large AWP years minus climatological mean, and (c) TC track density in small AWP years minus climatological mean. Based on the data from 1970 to 2009, the top and bottom quartiles of the ASO AWP index are identified as large and small AWP years, respectively.

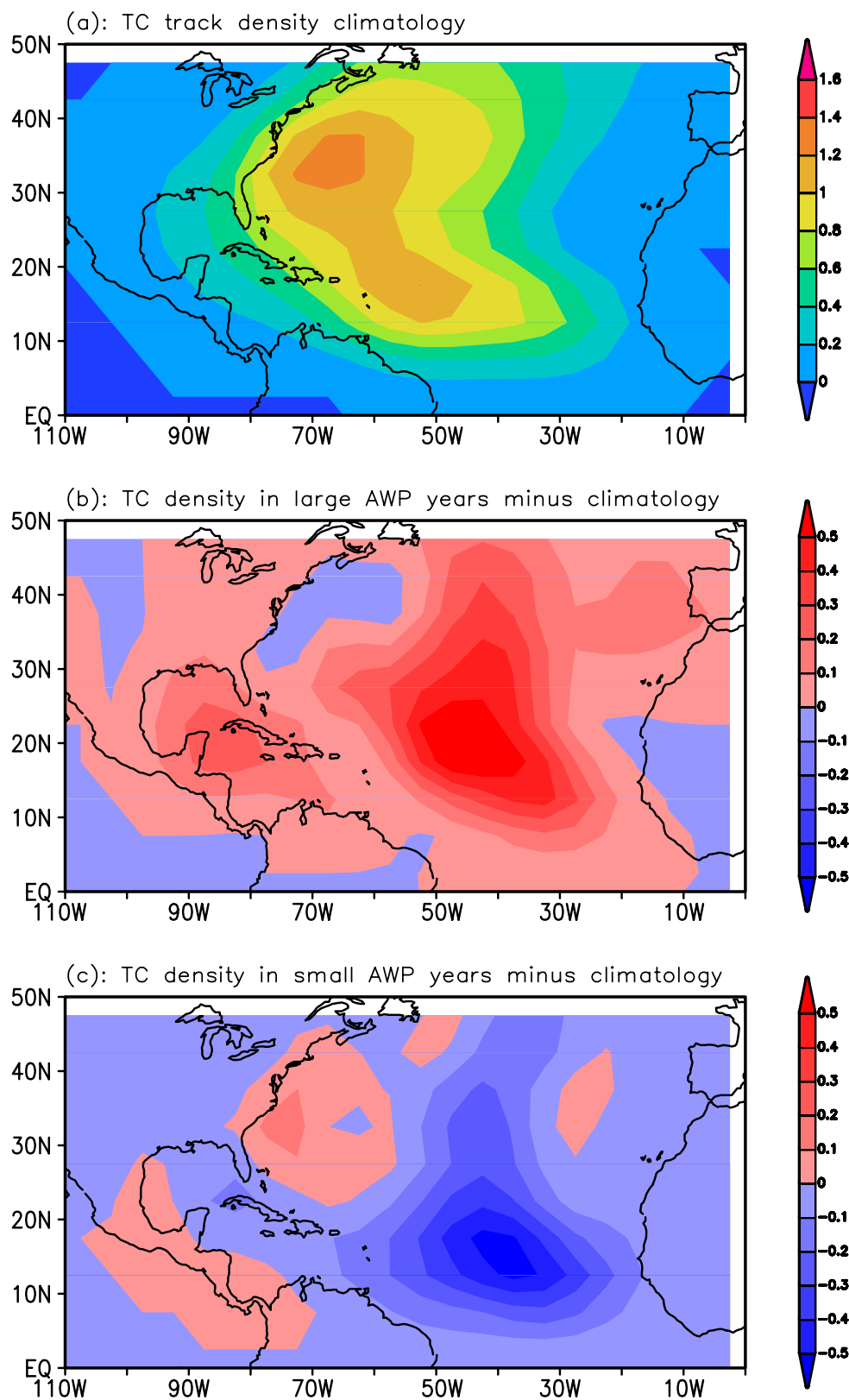


**Figure S3.** TC track density with IAS TCs excluded and AWP variability during ASO. Shown are (a) climatological TC track density, (b) TC track density in large AWP years minus climatological mean, and (c) TC track density in small AWP years minus climatological mean. Based on the data from 1970 to 2009, the top and bottom quartiles of the ASO AWP index are identified as large and small AWP years, respectively.

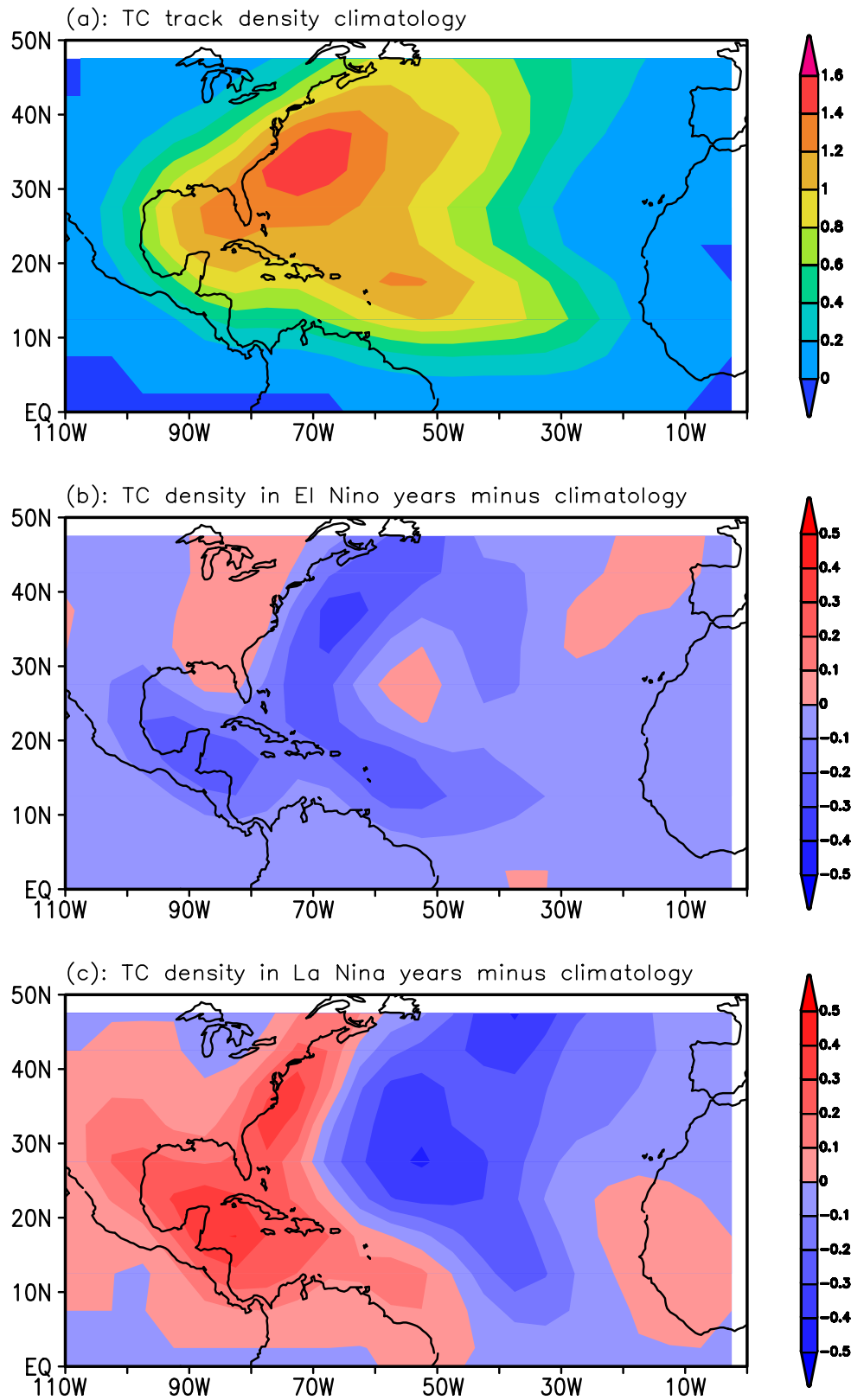


**Figure S4.** TC track density and ENSO variability during ASO. Shown are (a) climatological TC track density, (b) TC track density in El Niño years minus climatological mean, and (c) TC track density in La Niña years minus climatological mean. Based on the data from 1970 to 2009, El Niño and La Niña years are defined when the Niño3 SST anomalies are larger than  $\pm 0.5^{\circ}\text{C}$ , respectively.

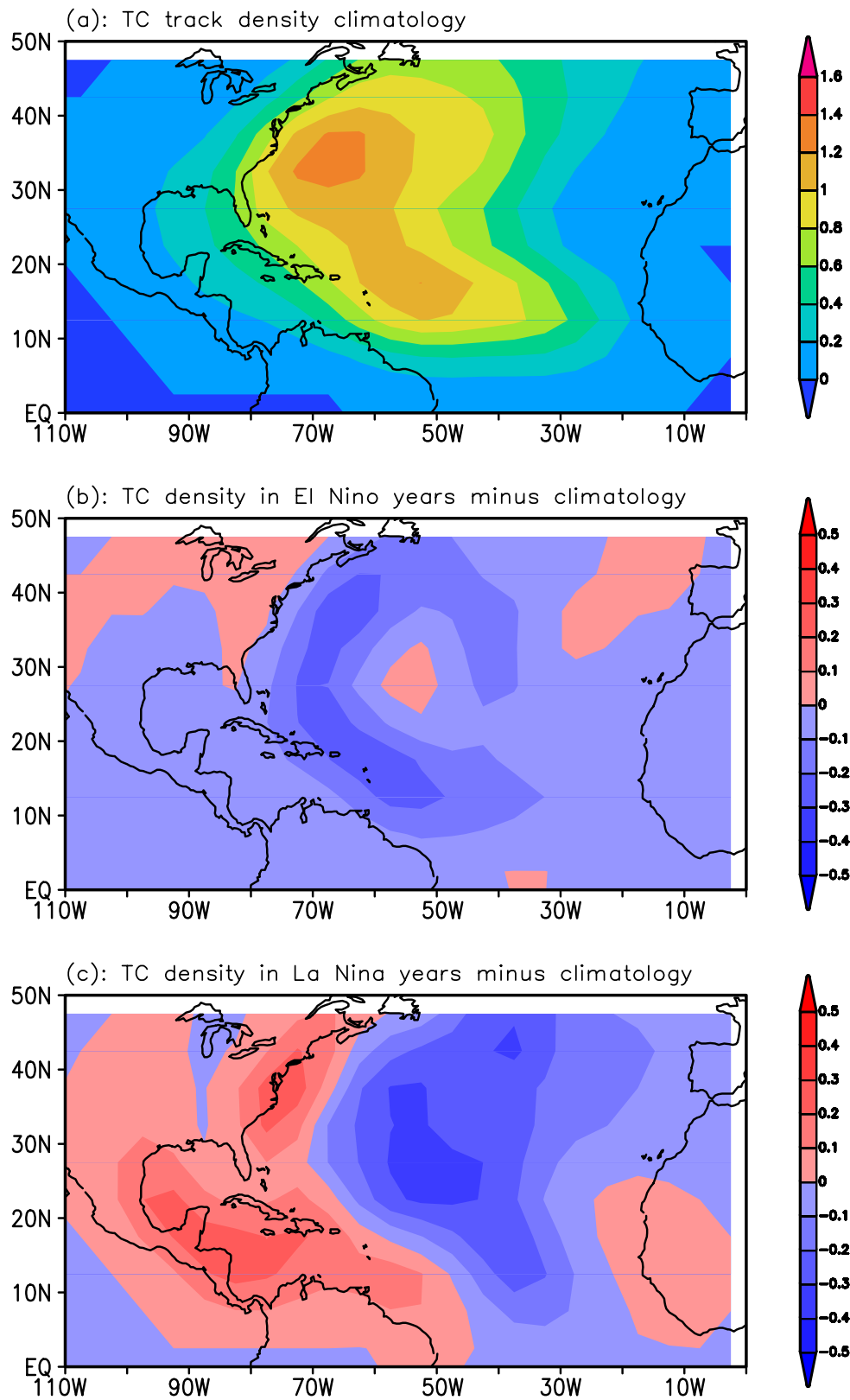


**Figure S5.** TC track density with IAS TCs excluded and ENSO variability during ASO. Shown are (a) climatological TC track density, (b) TC track density in El Niño years minus climatological mean, and (c) TC density in La Niña years minus climatological mean. Based on the data from 1970 to 2009, El Niño and La Niña years are defined when the Niño3 SST anomalies are larger than  $\pm 0.5^{\circ}\text{C}$ , respectively.

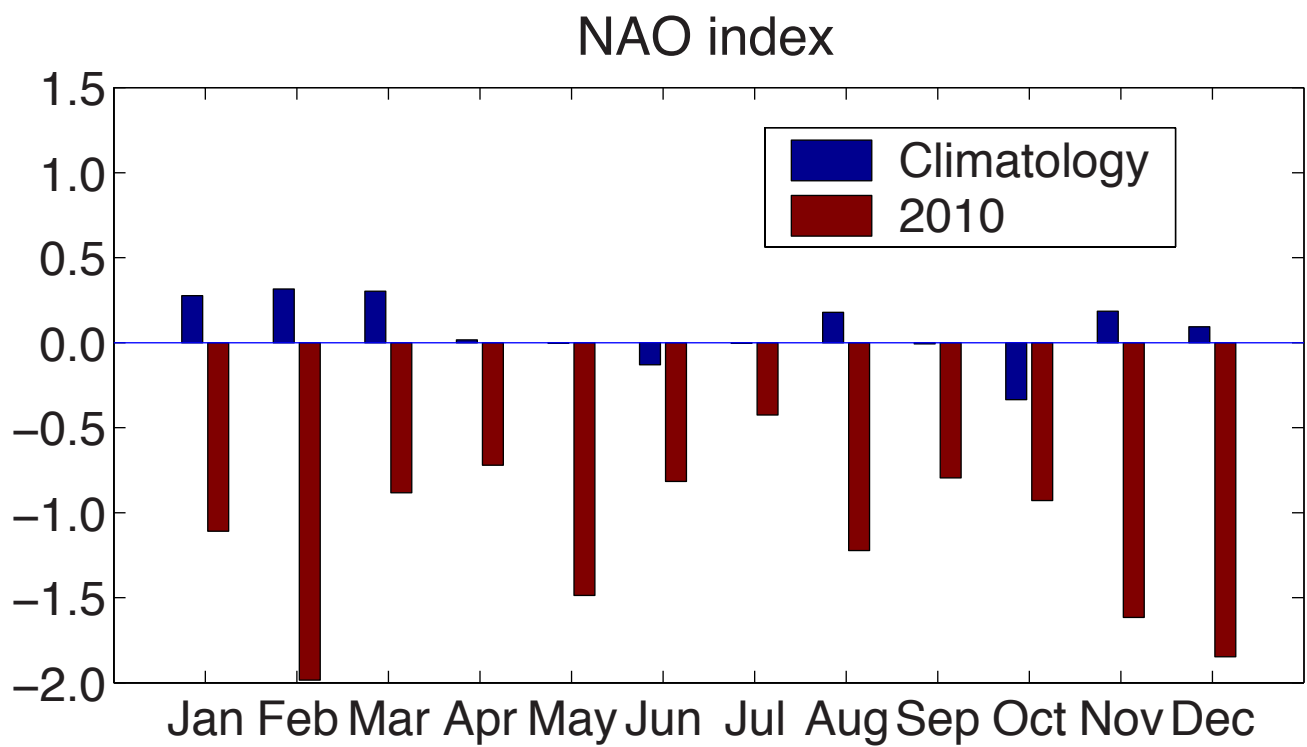


**Figure S6.** The North Atlantic oscillation (NAO) index. The red (blue) bars represent the 2010 (climatological) NAO index.

### HURDAT: Storm Track Density

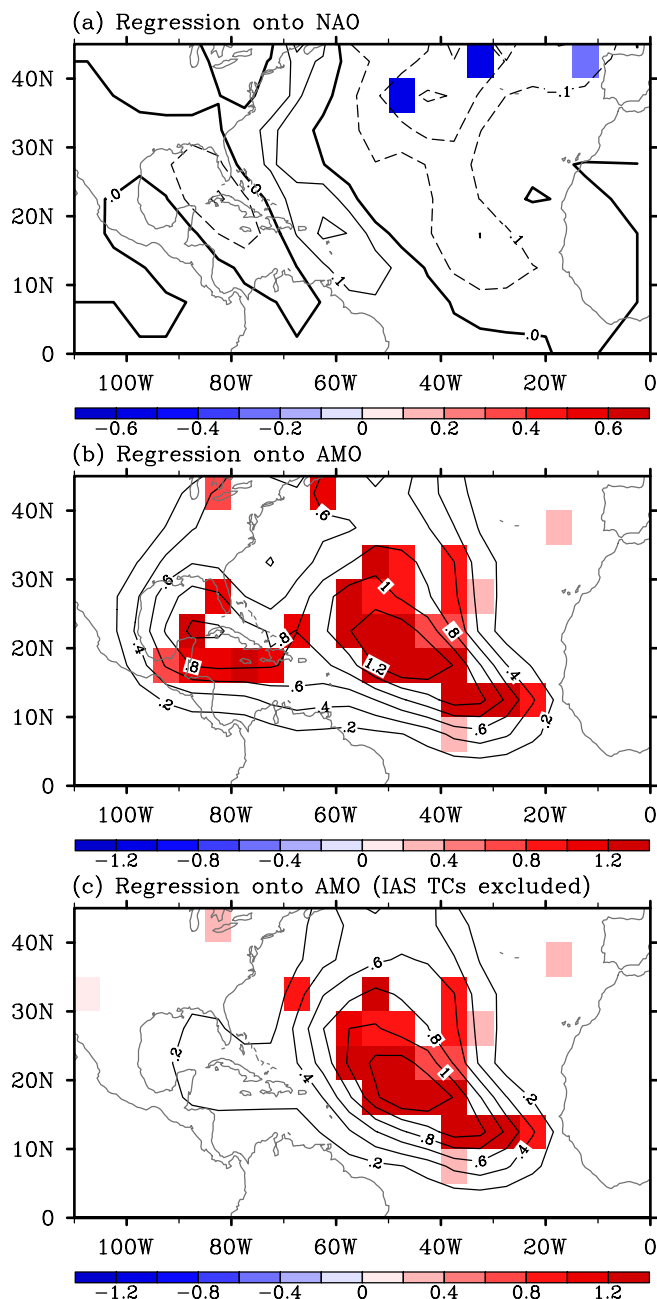


**Figure S7.** Relationships of TC track density with NAO and AMO variability during ASO. Shown are (a) the regression coefficient (the number per NAO index) of TC track density onto the NAO index, (b) the regression coefficient (the number per °C) of TC track density onto the AMO index, and (c) the regression coefficient (the number per °C) of TC track density onto the AMO index with IAS TCs excluded. The regression coefficients higher than the 95% significant level are shaded. The AMO index is computed by averaging the North Atlantic SST anomalies from the equator to 60°N.

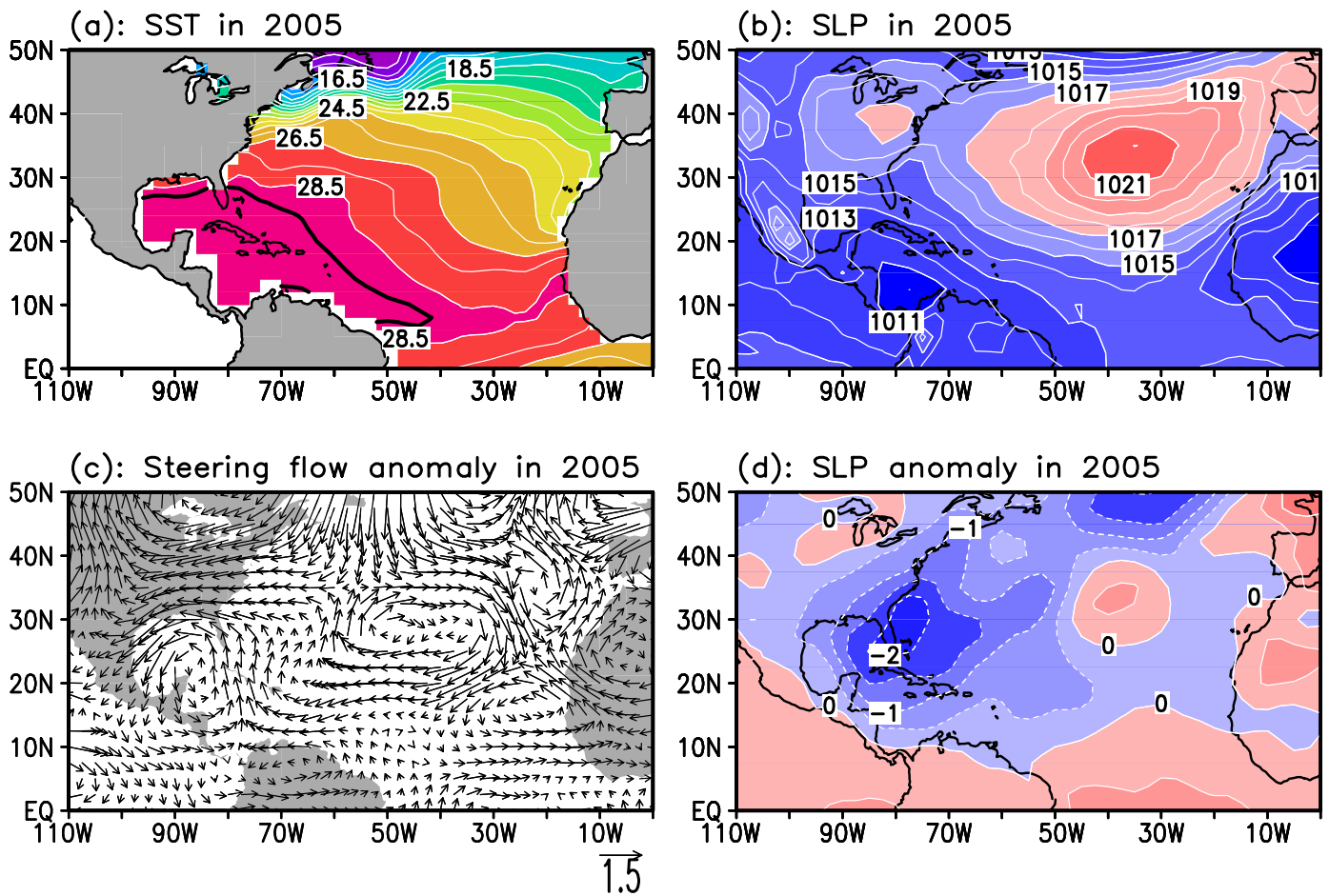
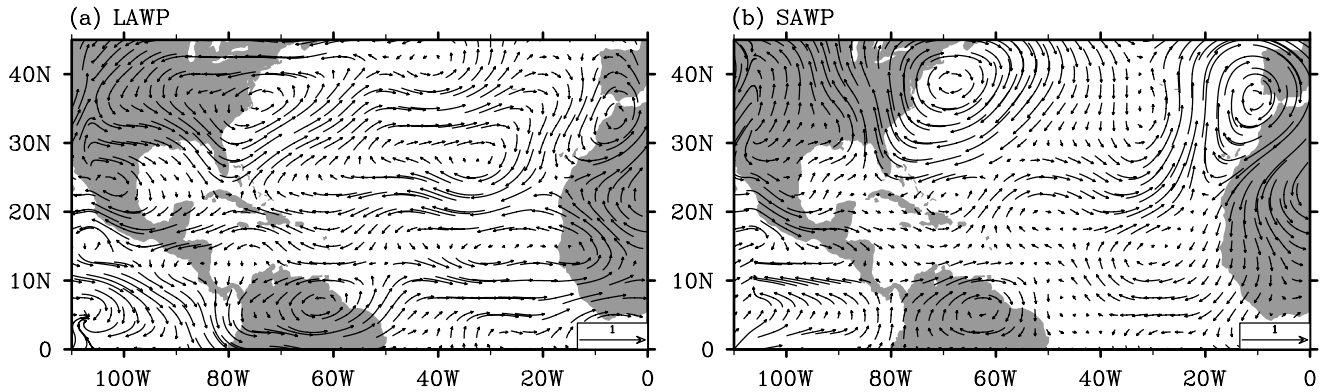


**Figure S8.** The AWP, NASH and steering flow during ASO of 2005. Shown are (a) the SST, (b) the SLP, (c) the steering flow anomalies ( $\times 103$  hPa m/s), and (d) the SLP in ASO of 2010 minus climatological ASO SLP. The AWP is defined by SST warmer than  $28.5^{\circ}\text{C}$ . The dark contour in (a) represents the climatological ASO AWP.

NCEP: Steering Flow



HURDAT: Storm Track Density

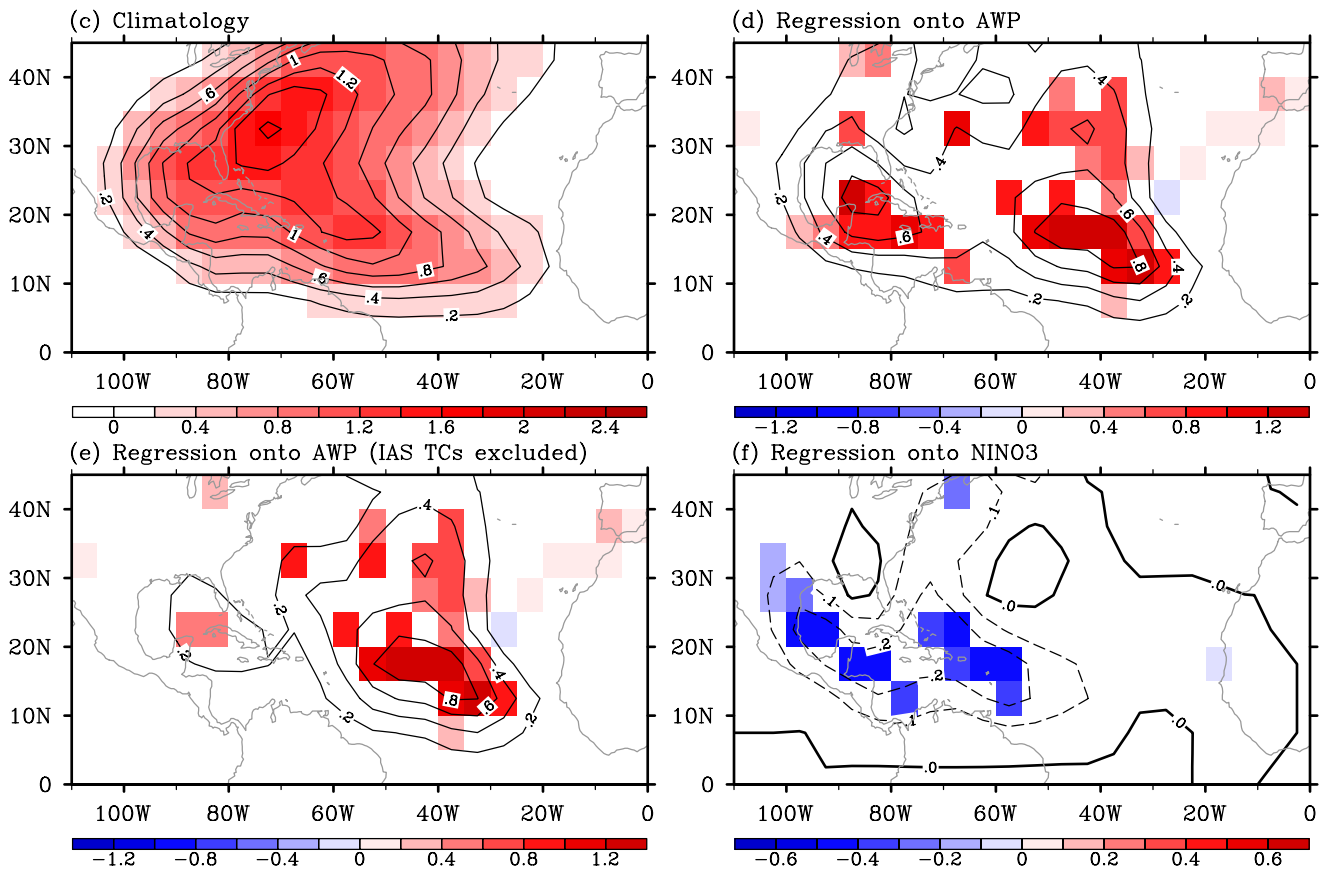


**Figure S9.** The relationships of the TC steering flow and TC track with climate variability using the data from 1950-2009. Shown are the TC steering flow anomalies ( $\times 10^3$  hPa m/s) for (a) large and (b) small AWP years, (c) the climatological mean of TC track density (the number), (d) the regression coefficient (the number per 100%) of TC track density onto AWP index, (e) the regression coefficient (the number per 100%) of TC track density onto AWP index with IAS TCs excluded, and (f) the regression coefficient (the number per  $^{\circ}\text{C}$ ) of TC track density onto Nino3 index. In (d)-(f), the regression coefficients higher than the 95% significant level are shaded. Based on the data from 1950 to 2009, the top and bottom quartiles of the ASO AWP index are identified as large and small AWP years, respectively. The 15 large AWP years are: 1958, 1969, 1987, 1990, 1998, 1999, 2001, 2002, 2003, 2004, 2005, 2006, 2007, 2008, and 2009 and the 15 small AWP years are: 1950, 1965, 1967, 1971, 1972, 1974, 1975, 1976, 1977, 1982, 1984, 1985, 1986, 1992, and 1994.